Figure 7. User costs over time.

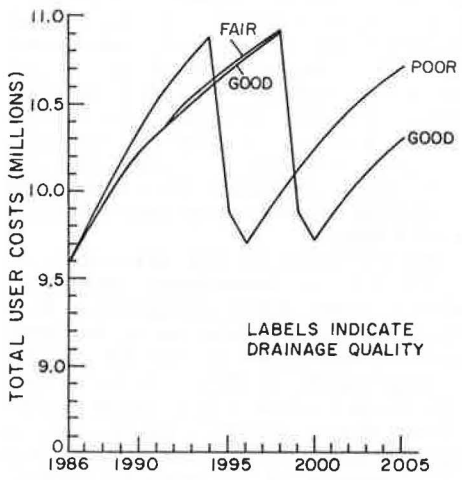

Table 2. Economic analysis of roadways with different drainage characteristics.

	Millions of Dollars				
Quality of Drainage	Overlay Expenditures	Maintenance Expenditures	User Costs	Total Costs	Cost Difference in Relation to Poor Drainage
Good	0.576	0.004	138.838	139.418	0.191
Fair	0.576	0.004	138.845	139.425	0.184
Poor	0.674	0.003	138.933	139.609	–

improve the drainage conditions or maintenance on the poor roadway. Stated another way, if the 10-mile roadway that has poor drainage could be rehabilitated to provide fair to good drainage or could be maintained each year to prevent water infiltration at a cost whose value discounted at 4 percent did not exceed $184 000 to $191 000, this improvement would be economically justified.

CONCLUSIONS

We have presented here an approach to assess the effects of drainage quality on pavement performance and costs. Although the procedure has been applied to date only within a simulation model and must yet be verified in the field, it provides a sound rational basis for organizing information on pavement structure, traffic and environmental loads, and damage accumulation with respect to water infiltration.

The results of our simulations indicate that, for flexible pavements in regions subject to annual rainfall of about 40 in (100 cm), the inclusion of good drainage characteristics within the pavement structure may increase acceptable performance life by about four years. On the other hand, poor drainage characteristics increase rates of rutting and roughness accumulation, decreasing overall pavement condition and increasing user costs for vehicle operation and travel time.

Further research is now under way to test this model for different pavements in different environmental regions and to assess the implications of maintenance policy on rates of damage influenced by water infiltration.

ACKNOWLEDGMENT

The research reported in this paper was supported by the Federal Highway Administration and the U.S. Department of Transportation's University Research Program. I gratefully acknowledge the support of these agencies and wish to thank in particular William J. Kenis, Contract Monitor, for his continued encouragement and assistance.

REFERENCES

1. H.R. Cedergren. Drainage of Highway and Airfield Pavements. Wiley, New York, 1974.
2. M.J. Markow and B.D. Brademeyer. Modification of System EAROMAR: Final Technical Report. FHWA, June 1981.
3. L.K. Moulton. Highway Subdrainage Design. FHWA, Rept. FHWA-TS-80-224, Aug. 1980.
4. H.L. Von Quintus, F.N. Finn, W.R. Hudson, and F.L. Roberts. Flexible and Composite Structures for Premium Pavements, Volume 1: Development of Design Procedure. FHWA, Rept. FHWA-RD-80, Nov. 1980.
5. AASHTO Interim Guide for Design of Pavement Structures. American Association of State Highway and Transportation Officials, Washington, DC, 1972.

Pumping Mechanisms of Foundation Soils Under Rigid Pavements

LUTFI RAAD

Pumping of foundation soils under rigid pavements is a soil structure interaction problem in which the interaction among traffic loads, concrete slab, pavement materials, and water should be considered. Repeated stress induced by moving wheel loads could result in pore-water pressures that reduce the strength and stiffness of underlying soil layers and lead to pumping and loss of foundation support. Pumping mechanisms of granular bases in rigid pavements are investigated in terms of dynamic pore-pressure generation and dissipation. Analyses are performed to study the significance of permeability and compressibility of base materials, loading conditions, and drainage conditions on pumping. Higher pore-pressure values are obtained as a result of decrease in base permeability or increase in its compressibility. The inclusion of lateral drains increases the rate of dynamic pore-pressure dissipation and therefore reduces the pumping potential of the granular base. The efficiency of lateral drains, however, is a function of loading frequency. Higher frequency of loading may not allow enough time for pore-pressure dissipation, which may lead to pumping of the base material. The significance of loss of foundation support on the structural response of the pavement is also studied. Results indicate that loss of foundation support leads to increased stresses and deflections in the concrete slab and therefore hastens its rate of deterioration.

Pumping is known to be a major cause of distress in concrete pavements. It occurs when the pore-water pressure buildup induced by heavy wheel loads is high enough to result in the ejection of material and water through cracks and joints in the pavement slab, causing loss of support and hastening the pavement's rate of deterioration.

Pumping of foundation soils under rigid pavements is a soil structure interaction problem in which the interaction among traffic loads, concrete slab, foundation materials, and water should be considered. Repeated stress states induced by moving wheel loads could result in pore-water pressures that reduce the strength and stiffness of underlying soil layers and lead to pumping and loss of foundation support.

Current design and evaluation techniques of subsurface drainage systems that are used to minimize pumping in pavements are based on the ability of these systems to drain pavement moisture under gravitational flow conditions. Permeability of the structural materials and drainage materials is the essential property that influences water drainage in this case. Loading effects imposed by moving traffic on pore-pressure generation and the effectiveness of subsurface drainage systems in dissipating the dynamic pore-pressure buildup have not yet been considered.

In this paper an attempt will be made to identify pumping mechanisms of granular bases in rigid pavements in terms of dynamic pore-water pressure generation and dissipation under repeated traffic loads. The influence of loading conditions, drainage conditions, and material properties on pumping will be investigated. The significance of pumping and the corresponding loss of foundation support on the structural response of the concrete slab will be illustrated.

DYNAMIC PORE-PRESSURE OBSERVATIONS UNDER RIGID PAVEMENTS

Pumping of foundation soils under rigid pavements is associated with dynamic pore-water pressure development under wheel loads. Repeated stress pulses could result in residual pore-water pressure buildup causing progressive loss of shear strength and stiffness in the underlying soil. Liquefaction of granular materials under the rigid slab occurs when the residual pore-water pressure becomes equal to the initial effective overburden pressure. Additional load repetitions could then result in the ejection of granular materials through cracks and joints in the pavement.

Liquefaction behavior of saturated granular soils has been investigated experimentally under undrained loading conditions by using cyclic triaxial tests (1). Thompson (2) performed repeated-load tests on two-dimensional pavement models consisting of a subgrade and a granular base. A transparent face on the model enabled visual observations of the subgrade and base materials. A high degree of saturation was obtained by soaking the pavements from top and bottom. Under repeated loading conditions, significant movements of the granular particles were observed directly under the loaded area. The entire base course within the loaded area appeared to liquefy and each load application caused a pumping action.

Large-scale tests performed on rigid pavement sections indicate that dynamic pore-water pressure could develop in the granular subbase when the pavement is subjected to repeated loads. Dempsey, Carpenter, and Darter (3) conducted repeated-load tests on two-dimensional rigid pavement models (Figure 1a). The sections were soaked and loaded at a frequency of 15 repetitions/min. Results of peak pore-water pressure (i.e., pore-water pressure at the peak of the load cycle) and residual pore-water pressure (i.e., pore-water pressure at the end of the load cycle) variations in a dense-graded base are shown in Figure 1b. An increase of pore pressure is observed with increase in number of load applications. Water and soil directly beneath the slab seemed to pump up along the sides of the slab and through the joint between the slab and the shoulder. Similar tests performed on open-graded bases showed no evidence of pumping or pore-pressure values in excess of 2 kPa.

Pilot tests were performed at the University of Illinois test track (3) to investigate pore-water pressure development under rigid pavements. This was part of a study entitled Evaluation of Drainage Systems for Pavements, sponsored by the New Jersey Department of Transportation (NJDOT). A test section consisting of 76-mm concrete slab, 76-mm dense-graded base, 102-mm clayey gravel subbase, and a clay subgrade was subjected to a 13.3-kN wheel load application at a frequency of 30 repetitions/min. The dynamic pore-water pressure at the interface between the slab and the base was monitored.

The variation of peak and residual pore pressure is shown in Figure 2. During the first loading sequence, an increase in peak and residual pore-pressure values is observed with increase in number of load repetitions. When loading stops, the residual pore pressure dissipates from 3.90 kPa to 1.70 kPa. Additional loading causes the pore pressure to build up again. In this case, peak pressure values are higher than those observed during the first loading sequence. This could be attributed to the development of voids under the slab and agrees with recent findings by Phu and Ray (4) that an increase in size of the cavity results in higher values of ejection velocity and therefore higher values of peak pore-water pressure.

DYNAMIC PORE-PRESSURE PREDICTIONS UNDER RIGID PAVEMENTS

The development of a pumping model requires an understanding of pore-water pressure development in soils under repeated stress applications similar to those induced by traffic loads. Martin and Seed (5) proposed a method for predicting pore-water pressure generation and dissipation in soils under dynamic loads. The basic assumption involved in their approach is that excess pore-water change in a soil element is the sum of the pore-pressure increment generated by repeated loading and the pore-pressure change due to drainage of water in and out of the element. Assuming one-dimensional flow (i.e., in the direction of the Z-axis) and applying Darcy's law, the basic differential equation for the simultaneous generation and dissipation of pore-water pressure can be written as follows:

$$(\partial u_r/\partial t) = [(1/m_v\gamma_w)(\partial u_r/\partial z)(k\partial u_r/\partial z)] + [(\partial u_g/\partial N)(dN/dt)] \quad (1)$$

where

γ_w = density of water,
u_r = residual pore-water pressure,
m_v = coefficient of volume compressibility,
k = permeability,
N = number of load repetitions,
$(\partial u_g/\partial N)$ = rate of generation of residual pore pressure under undrained loading condition, and
(dN/dt) = frequency of load applications.

Martin and Seed (5) used an implicit finite difference formulation to solve this equation. A com-

puterized form has been developed for pore-pressure predictions under rigid pavements and has been used in this study.

Analyses were performed to investigate dynamic pore-pressure development in soil layers underlying rigid pavements in terms of material properties, loading conditions, and drainage conditions. Stresses were computed in the pavement section and were used as input in pore-pressure prediction under traffic loads.

The finite-element method of analysis was used to determine the stresses in the pavement structure. Nonlinear stress-dependent behavior for the granular base and subgrade was incorporated in the analysis (6). For the granular base, the resilient modulus M_R can be expressed as follows:

$$M_R = K\theta^n \quad (2)$$

where

K, n = material constants,
$\theta = \sigma_1 + \sigma_2 + \sigma_3$, and
$\sigma_1, \sigma_2, \sigma_3$ = principal stresses for the following subgrade:

$$M_R = k_2 - k_3[k_1 - (\sigma_1 - \sigma_3)], \quad k_1 > (\sigma_1 - \sigma_3) \quad (3)$$

and

$$M_R = k_2 + k_1[(\sigma_1 - \sigma_3) - k_1], \quad k_1 < (\sigma_1 - \sigma_3) \quad (4)$$

where k_1, k_2, k_3, and k_4 are material constants. k_3 and k_4 are equal to the rate of change of M_R with repeated deviator stress $(\sigma_1 - \sigma_3)$.

The ratio of maximum shear stress τ_{max}, defined as $[(\sigma_1 - \sigma_3)/2]$, to the initial effective overburden pressure σ_0' was used to estimate the number of cycles required for initial liquefaction N_ℓ obtained from undrained cyclic triaxial tests (5). An example of the variation of N_ℓ with (τ_{max}/σ_0') for a uniform medium sand at different relative densities D_r is shown in Figure 3 (5). The dynamic pressure u_ℓ generated under undrained loading conditions was determined from the following expression (5):

$$u_\ell = \sigma_0' (2/\pi) \arcsin (N/N_\ell)^{(1/2\alpha)} \quad (5)$$

Figure 1. Dynamic pore pressure under rigid slab.

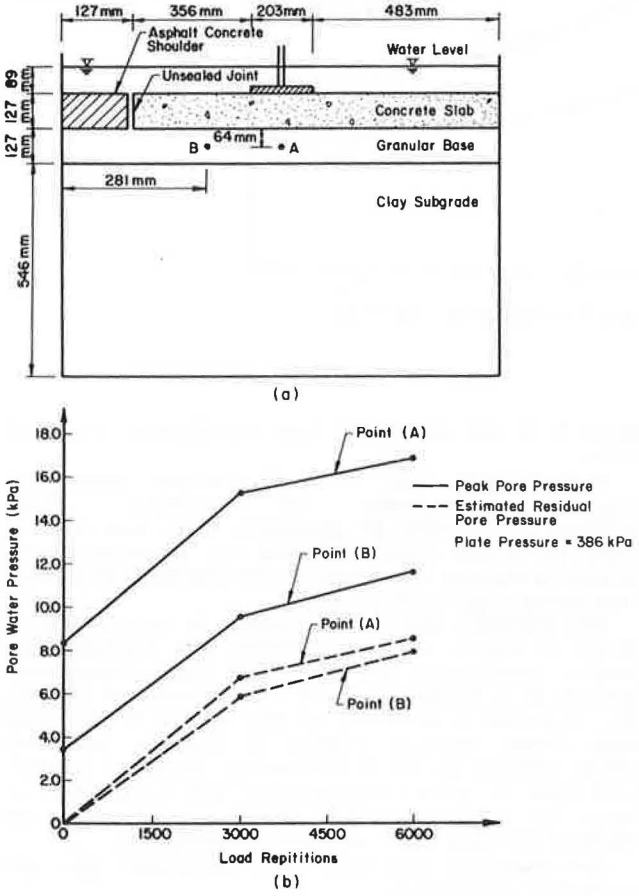

Figure 2. Dynamic pore pressure in dense-graded subbase.

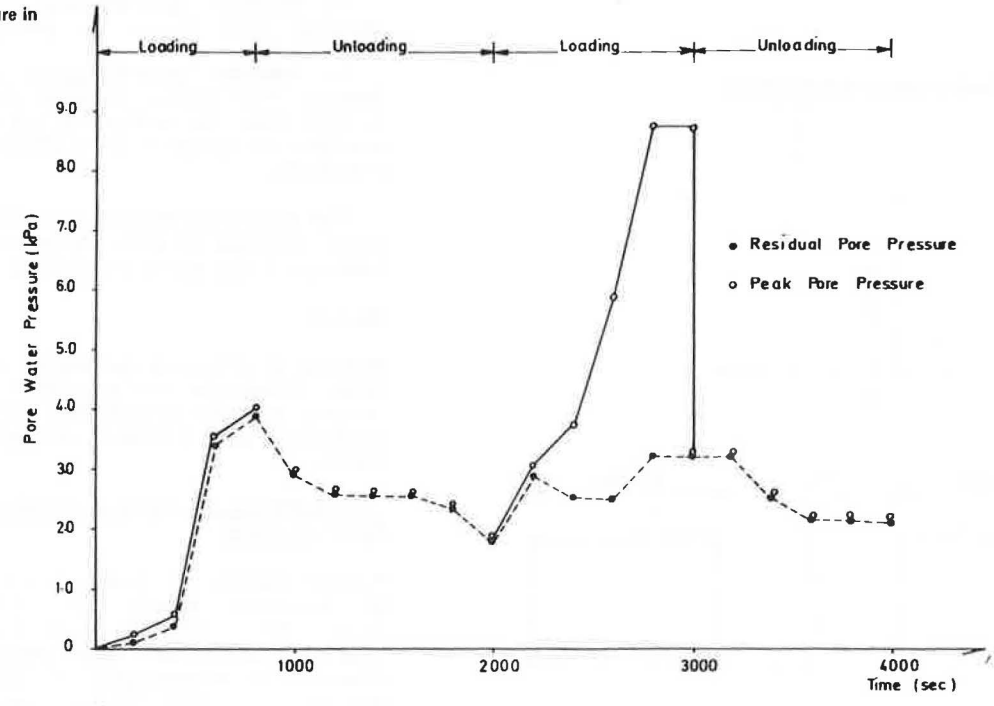

Figure 3. Typical cyclic loading test data.

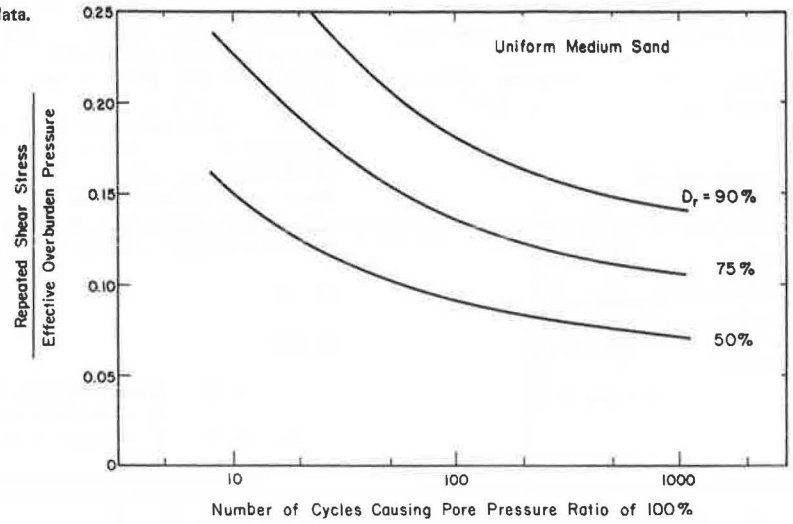

Figure 4. Pavement section analyzed.

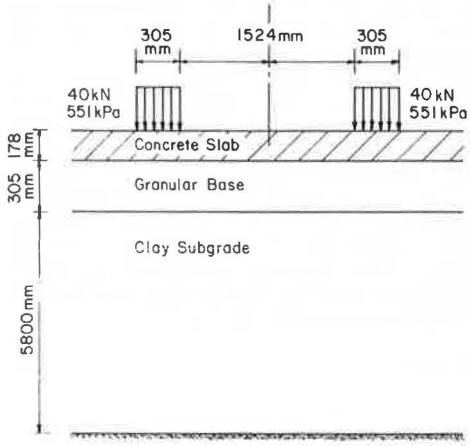

Figure 5. Loading sequence used in analyses.

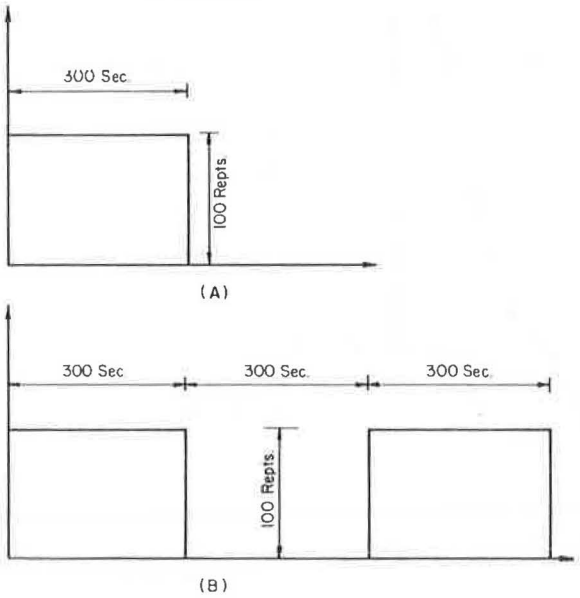

where N is the number of load repetitions and α is 0.70.

Knowing the rate of pore-pressure generation ($\partial u_g/\partial N$), frequency of applied loads (dN/dt), coefficient of permeability k, and coefficient of volume compressibility m_v, Equation 1 was solved to obtain the dynamic pore-pressure distribution under rigid pavements.

The pavement section considered in this study is shown in Figure 4. The pavement was subjected to loading sequences A and B of 80-kN single-axle loads applied at a frequency of 20 repetitions/min (Figure 5). Sequence A consists of one series of 100-load repetitions, whereas sequence B includes two such series applied at 300-s intervals. Material properties used in stress computations are summarized in Table 1. The variation of (τ_{max}/σ_0') in the pavement section is illustrated in Figure 6.

Pore-pressure analyses were performed for the following conditions:

1. Dynamic pore-pressure dissipation through vertical flow (i.e., no lateral drainage is allowed); and
2. Dynamic pore-pressure dissipation through lateral flow (i.e., lateral drainage is allowed). In this case the efficiency of subsurface drains in dissipating dynamic pore-water pressure could be evaluated.

The finite-difference representation of the sections analyzed is illustrated in Figures 7 and 8. A summary of the cases studied is presented in Table 2.

RESULTS

Results of analyses presented in the following sections illustrate the significance of material properties, loading conditions, and drainage conditions on dynamic pore pressure and pumping in rigid pavements.

Pore-Pressure Dissipation Through Vertical Flow

Dynamic pore-water pressure was calculated assuming pore-pressure dissipation through vertical flow (i.e., no lateral drainage was allowed). Higher pore-pressure values were obtained as a result of decrease in permeability of the granular base. For example, a pore-pressure ratio [i.e., u_r/σ_0']

equal to unity will develop if the permeability decreases from 10^{2} to 10^{-2} cm/s (Figure 9, cases 1 and 2). In this case the pore pressure becomes equal to the initial effective overburden pressure and a condition of initial liquefaction will occur, thereby increasing the susceptibility of the granular base to pumping. Similar behavior is observed for higher compressibility of the base (cases 2 and 3) or larger number of load repetitions (cases 2 and 4).

The effect of permeability and compressibility of

Table 1. Material properties used in stress predictions.

Material	Resilient Properties	Failure Criteria	Density (kg/m^3)
Concrete	$E = 34.5 \times 10^6$ kPa $\nu = 0.10$	—	2400
Base course	$K = 6495$ $n = 0.60$ $\nu = 0.30$	$C = 0$ $\phi = 30^0$	2130
Subgrade	$k_1 = 41.3$; $k_2 = 41\,300$ $k_3 = 0.300$; $k_4 = -75$ $\nu = 0.45$	$C = 90$ kPa $\phi = 0^0$	1950

Notes: Saturated unit weights are used for base course and subgrade. K,n are parameters for resilient modulus of base course (Equation 2). k_1, k_2, k_3, k_4 are parameters for resilient modulus of subgrade (Equations 3 and 4). Resilient moduli of base and subgrade are expressed in kilopascals. E and ν are elastic modulus and Poisson's ratio, respectively.

Figure 6. Variation of maximum shear with depth under center of wheel load.

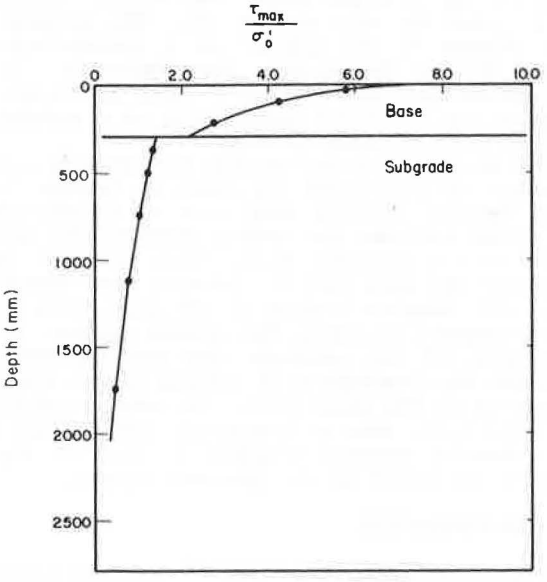

Figure 7. Finite difference representation for vertical flow condition.

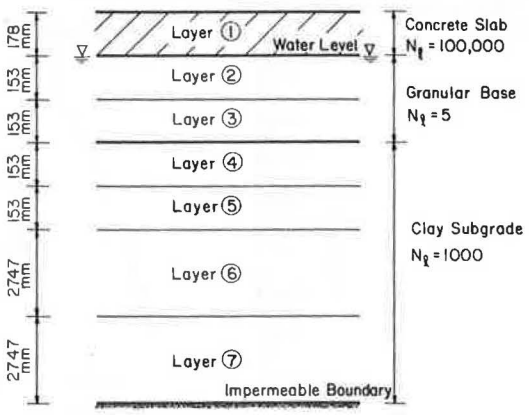

Figure 8. Finite difference representation for lateral flow condition.

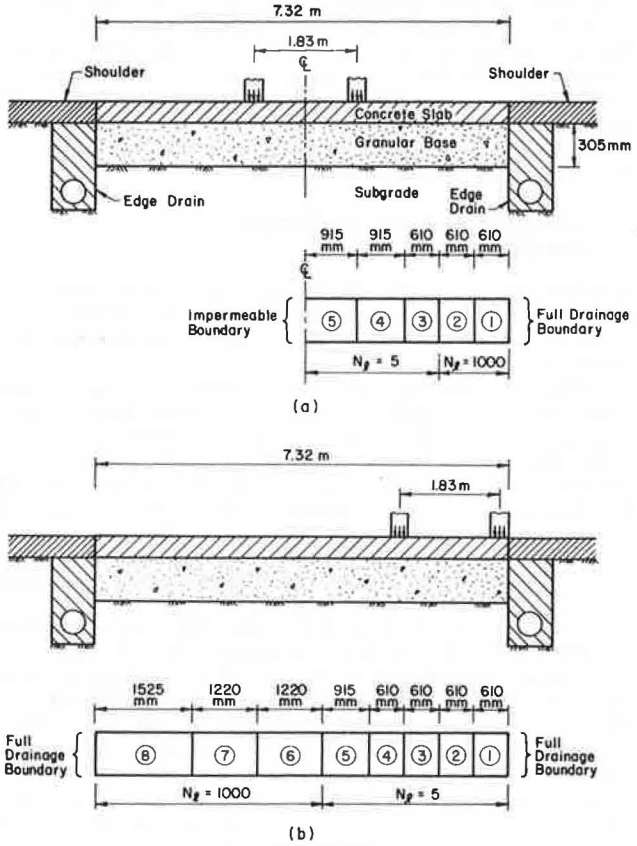

Table 2. Pavement systems analyzed.

Case	Concrete k (cm/s)	Concrete m_v (m^2/kN)	Base Course k (cm/s)	Base Course m_v (m^2/kN)	Subgrade k (cm/s)	Subgrade m_v (m^2/kN)	Loading Sequence	Drainage Condition
1	10^{-8}	2.0×10^{-7}	10^{-2}	2.0×10^{-5}	10^{-8}	2.0×10^{-4}	A	Vertical flow
2	10^{-8}	2.0×10^{-7}	10^{-2}	2.0×10^{-5}	10^{-8}	2.0×10^{-4}	A	
3	10^{-8}	2.0×10^{-7}	10^{-2}	2.0×10^{-4}	10^{-8}	2.0×10^{-4}	A	
4	10^{-8}	2.0×10^{-7}	10^{-2}	2.0×10^{-5}	10^{-8}	2.0×10^{-4}	B	
5	—	—	10^{-1}	2.0×10^{-5}	—	—	A	Lateral flow (interior loading)
6	—	—	10^{-2}	2.0×10^{-5}	—	—	A	
7	—	—	10^{-2}	2.0×10^{-4}	—	—	A	
8	—	—	10^{-2}	2.0×10^{-4}	—	—	B	
9	—	—	10^{-1}	2.0×10^{-5}	—	—	A	Lateral flow (edge loading)
10	—	—	10^{-2}	2.0×10^{-5}	—	—	A	
11	—	—	10^{-2}	2.0×10^{-4}	—	—	A	
12	—	—	10^{-2}	2.0×10^{-4}	—	—	B	

Note: Relative density D_r of granular base is 85 percent.

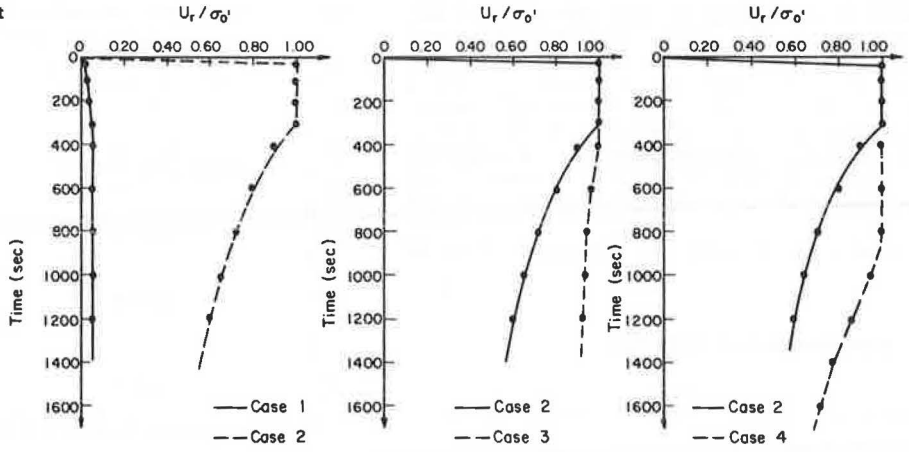

Figure 9. Dynamic pore pressure at top of granular base for pavement with no lateral drainage.

the base on pore-pressure dissipation at the end of a loading sequence is illustrated in Figure 10. Higher values of pore pressure are maintained for longer periods of time as a result of decrease in base permeability or increase in its volume compressibility. This would increase the pumping potential of the base if the pavement is subjected to an additional sequence of loads.

Pore-Pressure Dissipation Through Lateral Flow

Results of analyses performed to investigate the effectiveness of subsurface drains in dissipating dynamic pore pressure under rigid pavements are shown in Figures 11-14.

Interior loading of the pavement (Figure 11) could result in pumping of the granular base [i.e., $(u_r/\sigma_0') = 1$] provided its permeability is less than 10^{-2} cm/s. An increase in volume compressibility of the base from 2.0×10^{-3} m²/kN to 2.0×10^{-4} m²/kN would reduce the rate of pore-pressure dissipation as illustrated in Figures 11 and 12 (cases 6 and 7). Additional load applications would increase the pore pressure in the base and may cause additional pumping (Figure 12c).

Similar observations are made for loads applied at the edge of the slab (Figures 13 and 14). In this case, however, a reduction in permeability from 10^{2} to 10^{-2} cm/s would not cause pumping as shown in Figures 13 and 14 (cases 9 and 10). This could be attributed to the effectiveness of subsurface drains in dissipating the dynamic pore pressures induced by such loading conditions. If this reduction in permeability is accompanied by an increase in volume compressibility to a value of 2.0×10^{-4} m²/kN, then the pore-pressure ratio would increase from 0.3 to 1.0 (Figures 13c and 14b) and pumping of the granular base could occur.

The effectiveness of subsurface drains in dissipating dynamic pore pressure and therefore in reducing pumping potential is illustrated by comparing results in Figures 9 and 12. For the same material properties and loading conditions, the rate of pore-pressure dissipation is greater for pavements with subsurface drains.

The efficiency of subsurface drains depends to a certain extent on the frequency of load applications. A decrease in frequency of loading would increase the time span between load applications, thereby allowing more time for pore-pressure dissipation. Higher frequency of loading may not allow enough time for pore-pressure dissipation and therefore could lead to initial liquefaction and pumping.

STRUCTURAL EFFECTS

The development of excess pore-water pressure under rigid pavements reduces the effective stresses and leads to a decrease in shear strength and stiffness of pavement materials. Loss of foundation support could result from increased permanent deformations or pumping of foundation material through cracks and joints in the pavement.

Analyses were performed to investigate the effect of loss of foundation support on the structural response of the concrete slab. The finite-element method was used for this purpose (7). The pavement section (Figure 5) was modeled as a medium-thick plate on a Winkler foundation. The modulus of subgrade reaction used was 52 MN/m³. Loss of foundation support was simulated analytically by a modulus of subgrade reaction equal to zero.

Tensile stresses and deflections for interior and edge-loading (8) conditions are shown in Figures 15 and 16. Results indicate that loss of foundation support would increase the tensile stresses and deflections in the pavement slab. This increase is more critical for edge than for interior load applications. For interior loading of the slab, loss of foundation support increases the tensile stresses on the underside of the pavement slab and therefore could hasten the development of fatigue cracks along the direction of the wheel path. For edge loading, on the other hand, loss of foundation support could induce excessive tensile stresses on top of the slab, which may result in edge punchout failure.

SUMMARY AND CONCLUSIONS

In this paper, pumping mechanisms of granular bases in rigid pavements have been investigated in terms of dynamic pore-water pressure generation and dissipation under repeated traffic loads. Dynamic pore-pressure development reduces shear strength and stiffness of underlying soil layers. Liquefaction of saturated granular materials under the rigid slab occurs when the residual pore-water pressure becomes equal to the initial effective overburden pressure. Additional load repetitions could then result in the ejection of base material through cracks and joints in the pavement.

Analyses were performed to study the significance of permeability and compressibility of base materials, loading conditions, and drainage conditions on pumping. Higher pore-pressure values were obtained as a result of a decrease in base permeability or an increase in its compressibility. The inclusion of lateral drains increases the rate of dynamic pore-

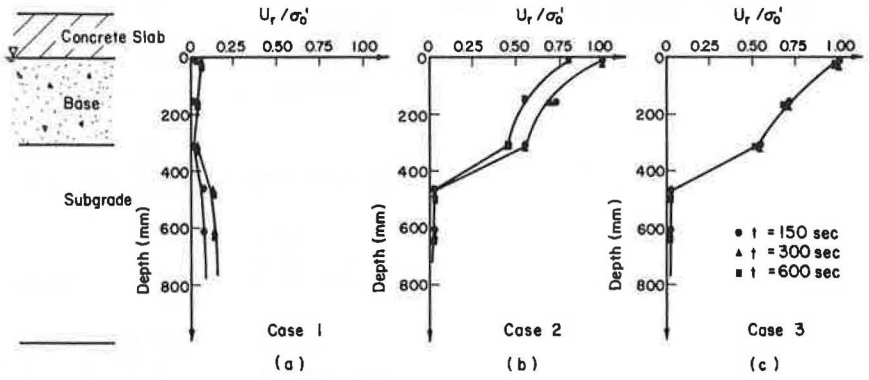

Figure 10. Dynamic pore-pressure variation below center of wheel load for pavement with no lateral drainage.

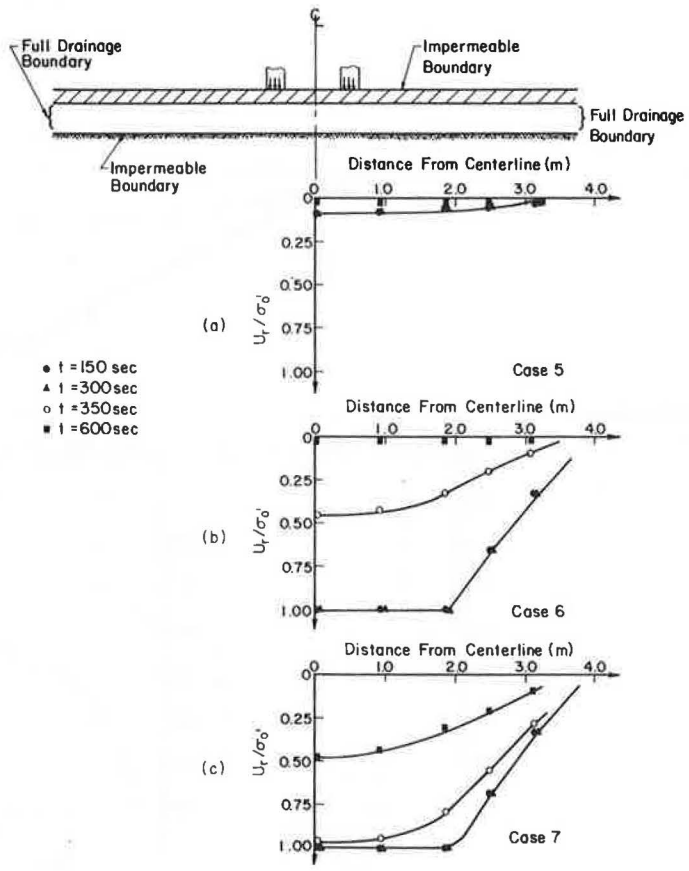

Figure 11. Pore-pressure variation for interior loading of slab.

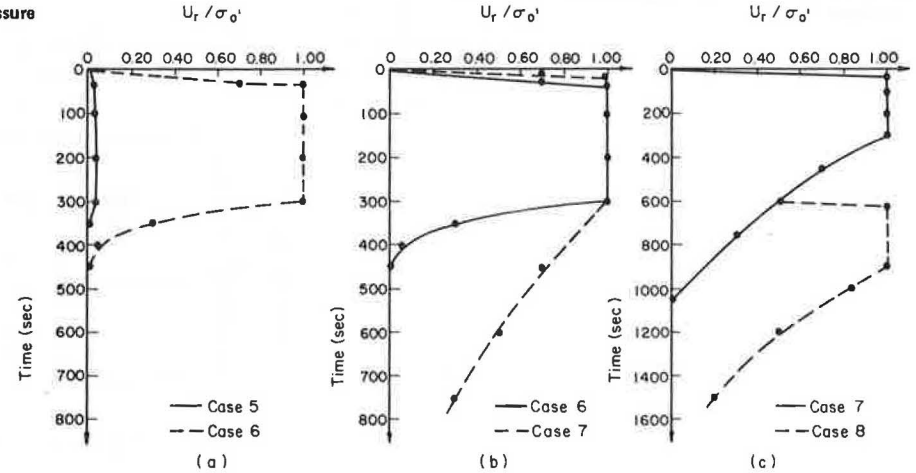

Figure 12. Variation of maximum pore pressure in base for interior loading of slab.

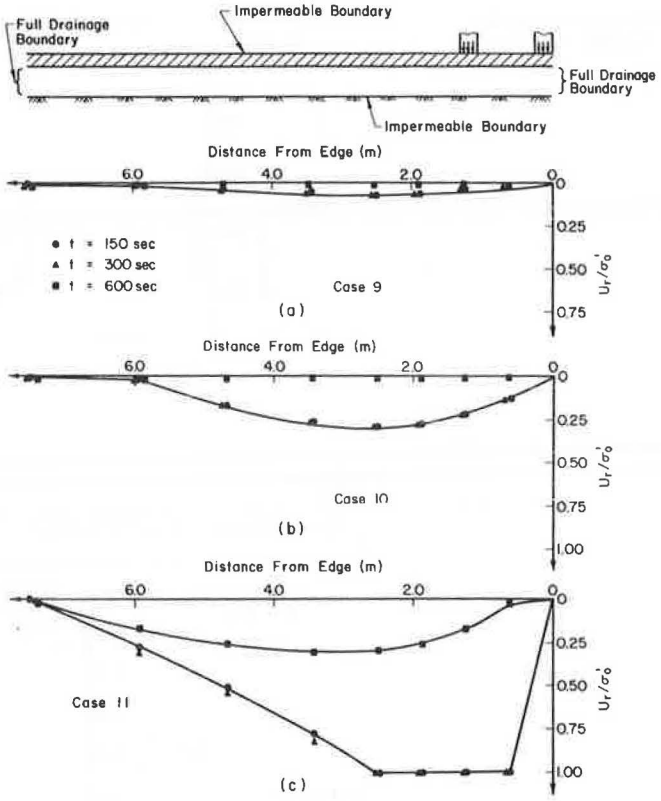

Figure 13. Pore-pressure variation for edge loading of slab.

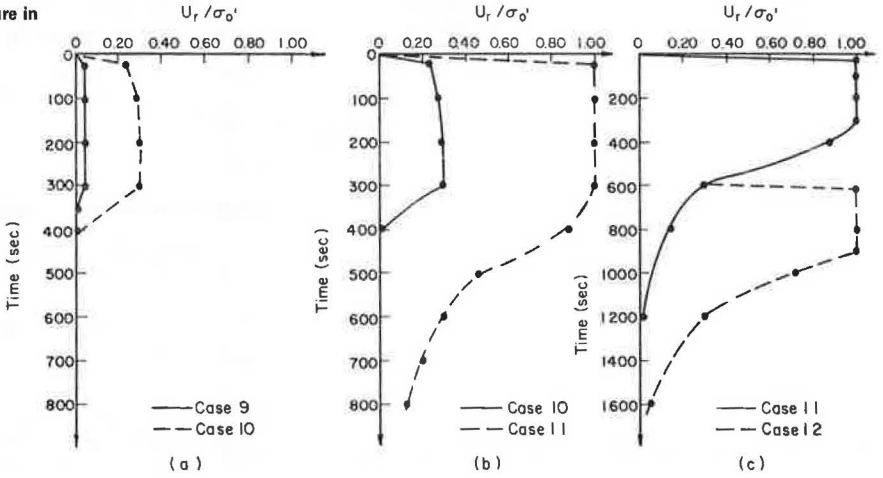

Figure 14. Variation of maximum pore pressure in base for edge loading of slab.

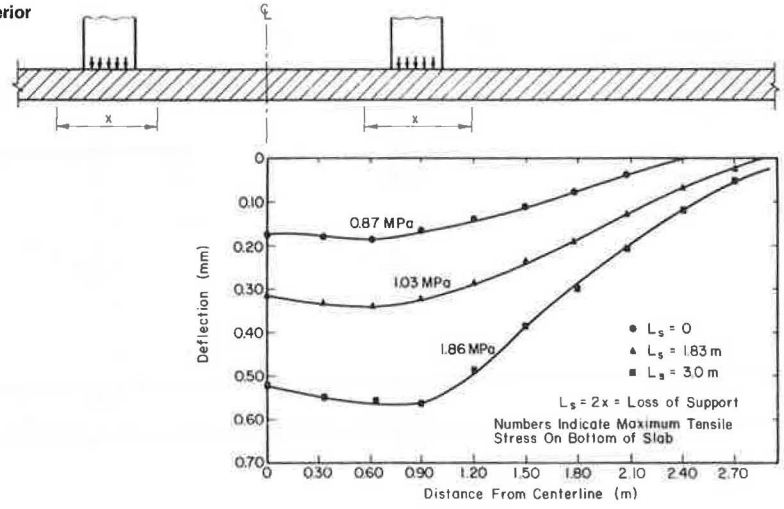

Figure 15. Effect of loss of support on slab response for interior loading condition.

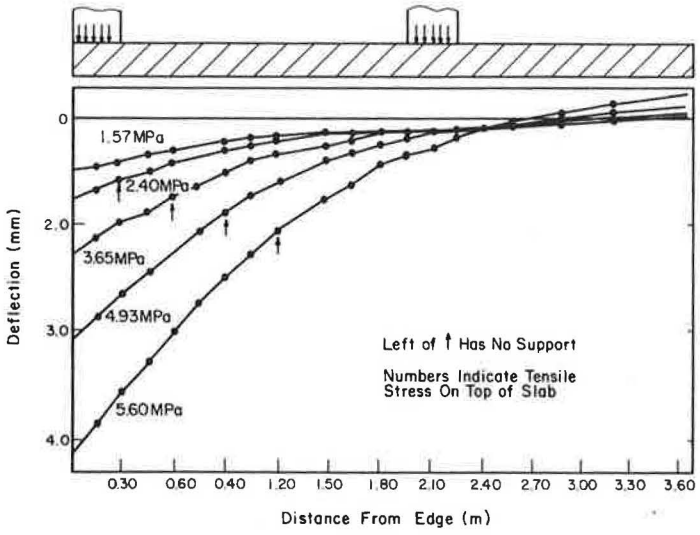

Figure 16. Effect of loss support on slab response for edge loading condition.

pressure dissipation and therefore reduces the pumping potential of the granular base. The efficiency of lateral drains, however, is a function of loading frequency. Higher frequency of load applications would not allow enough time for pore-pressure dissipation, which could lead to pumping of base material.

Results of analyses indicate that loss of foundation support caused by pumping and permanent deformations of soil layers under the pavement would result in increased stresses and deflections in the concrete slab and therefore would hasten its rate of deterioration.

ACKNOWLEDGMENT

This investigation was conducted at the University of Illinois at Urbana-Champaign. I appreciate the assistance of B.J. Dempsey and E.J. Barenberg in conducting the pilot tests at the University of Illinois test track. Special thanks go to P.P. Martin and H.Y. Chu for their help during the analytical studies.

REFERENCES

1. H.B. Seed and K.L. Lee. Liquefaction of Saturated Sands During Cyclic Loading. Journal of Soil Mechanics and Foundation Engineering of ASCE, Vol. 92, No. SM6, Nov. 1966, pp. 105-134.
2. O.O. Thompson. Evaluation of Flexible Pavement Behavior with Emphasis on the Behavior of Granular Layers. Department of Civil Engineering, Univ. of Illinois at Urbana-Champaign, Ph.D. thesis, 1969.
3. B.J. Dempsey, S.H. Carpenter, and M.I. Darter. Improving Subdrainage and Shoulders of Existing Pavements. FHWA, Final Rept., Aug. 1980.
4. N.C. Phu and M. Ray. Hydraulique du Pompage des Chaussees en Beton Premier Bilan de l'Approche Theorique et des Resultats de Mesure en Laboratoire et sur Autoroute. Chaussées en Beton, Laboratoire Central des Ponts et Chaussées, Paris, 1979, pp. 15-31.
5. P.P. Martin and H.B. Seed. APOLLO: A Computer Program for the Analysis of Pore Pressure Generation and Dissipation in Horizontal Sand Layers During Cyclic or Earthquake Loading. Univ. of California, Berkeley, Rept. UCB/EERC-78/21, Oct. 1978.
6. L. Raad and J.L. Figueroa. Load Response of Transportation Support Systems. Transportation Engineering Journal of ASCE, Vol. 106, No. TE1, Jan. 1980, pp. 111-128.
7. A.M. Tabatabaie, E.J. Barenberg, and R.E. Smith. Analysis of Load Transfer Systems for Concrete Pavements, Volume 2: Analysis of Load Transfer Systems in Concrete Pavements. Federal Aviation Administration, U.S. Department of Transportation, 1979.
8. S.A. LaCoursiere, M.I. Darter, and S.A. Smiley. Performance of Continuously Reinforced Concrete Pavements in Illinois. FHWA, Rept. FHWA-IL-UI-112, Dec. 1979.